HTML ABSTRACT + LINKS

Enhanced low field magnetoresistance of Al_2O_3-$La_{0.7}Sr_{0.3}MnO_3$ composite thin films via a pulsed laser deposition

L. Yan[a)]
Center for Superconducting and Magnetic Materials, Department of Physics, Faculty of Science, National University of Singapore, Lower Kent Ridge Crescent, Singapore 119260, Singapore

L. B. Kong[b)]
Temasek Laboratories, National University of Singapore, 10 Kent Ridge Crescent, Singapore 119260, Singapore

T. Yang, W. C. Goh, C. Y. Tan, and C. K. Ong
Center for Superconducting and Magnetic Materials, Department of Physics, Faculty of Science, National University of Singapore, Lower Kent Ridge Crescent, Singapore 119260, Singapore

Md. Anisur Rahman, T. Osipowicz, and M. Q. Ren
Centre for Ion Beam Applications, Department of physics, National University of Singapore, Lower Kent Ridge Crescent, Singapore 119260, Singapore

(Received 23 January 2004; accepted 28 April 2004)

Al_2O_3-doped $La_{0.7}Sr_{0.3}MnO_3$(Al_2O_3-LSMO) thin films were deposited on Si(111) substrate via a pulsed laser deposition. The deposited Al_2O_3-LSMO composite thin films were characterized by x-ray diffraction, scanning electron microscopy, and electro- and magneto-transport measurements. The main phase in the Al_2O_3-LSMO composite films was the perovskite phase. Texturelike microstructure was observed in the Al_2O_3-LSMO composite films while the average grain size remained almost unchanged compared to the pure samples. The metal-insulator transition temperature decreased as a result of the addition of Al_2O_3 and further reduced with increasing Al_2O_3 content. A maximum low field mangetoresistance of ~15% was achieved in the 2/20 Al_2O_3 -LSMO thin films, which could be well explained in terms of the grain boundary tunneling effect. The composition of the composite thin films can be easily tuned by adjusting the target composition. This method is believed to be applicable to exploring the combinations of other manganites and insulators. © *2004 American Institute of Physics*. [DOI: 10.1063/1.1763237]

I. INTRODUCTION

Since the discovery of "colossal magnetoresistance" (CMR) in perovskite based rare-earth manganites of the type $Ln_{1-x}A_xMnO_3$ (Ln is rare earth, A is divalent cation), intense research activities have been focused on these materials over the last few years.[1–5] However, the intrinsic CMR effect in the perovskite manganites is only triggered at high magnetic fields of several tesla, which restrains its use for practical applications. Therefore, it is desired to explore materials with low field magnetoresistance (LFMR). The fact that a low external magnetic field of the order of the coercive field H_c can yield large variations in the resistance at low temperatures in polycrystalline manganites is due to the presence of the high values of spin polarization[6] and most likely pinning of domain walls at the grain boundaries.[7] In this respect, LFMR is an extrinsic property of manganites and has been mainly attributed to the grain boundary magnetroresistance (GBMR). The GBMR is usually thought to be a result of the spin polarized tunnelling through electronic barriers at the grain boundaries. Hence, artificial grain boundary effect can be realized by proper incorporation of dopant into manganites.

Various attempts have been made to increase the LFMR effect of perovskite manganites by doping. For instance, Gupta *et al.*[8] reported enhanced mangnetoresistance in $La_{0.7}Sr_{0.3}MnO_3$-glass composites. They attributed the enhanced MR to the presence of a glass layer at the grain boundaries separating the manganite grains and thus enhancing the LFMR. Similar results were also observed in other systems of manganite-insulator composites. They include $La_{2/3}Ca_{1/3}MnO_3$-Al_2O_3,[9] $La_{1-x}Ca_xMnO_3$-ZrO_2,[10] $La_{2/3}Sr_{1/3}MnO_3-CeO_2$,[11,12] $La_{0.67}Ca_{0.33}MnO_3$-$SrTiO_3$,[13,14] and $La_{0.67}Ba_{0.33}MnO_3$-YSZ.[15] However, these strategies have been mostly applied to bulk ceramics or screen-printed thick films. Thin films are more favorable for electronic applications. To date, very few examples of thin films have been reported in the literatures regarding the enhanced LFMR effect in manganite thin films. Moshnyaga *et al.*[16,17] reported $La_{0.7}Ca_{0.3}MnO_3$-MgO composite thin films deposited via a sol-gel process. Liu *et al.*[18] found enhanced LFMR in partially crystallized $La_{0.5}Sr_{0.5}MnO_3$ thin films by laser ablation deposition at an optimized deposition temperature, where amorphous LSMO served as an insulating matrix separating the crystallized magnetic LSMO crystal grains. Exploring other ways to increase the LFMR effect will always be of both technological and scientific significances.

In this paper, we report an alternative way to produce LFMR $La_{0.7}Sr_{0.3}MnO_3$(LSMO) thin films with the addition

[a)]Electronic mail: iesyl@nus.edu.sg
[b)]Electronic mail: tslklb@nus.edu.sg

 © 2004 American Institute of Physics

Downloaded 29 Jul 2004 to 137.132.123.76. Redistribution subject to AIP license or copyright, see http://jap.aip.org/jap/copyright.jsp

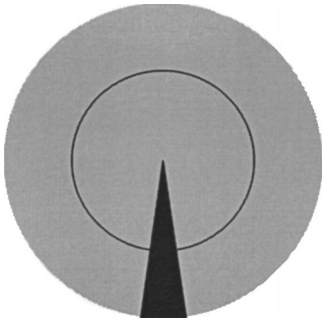

FIG. 1. Representative target configuration of Al_2O_3 (dark area) and LSMO (gray area) ceramics.

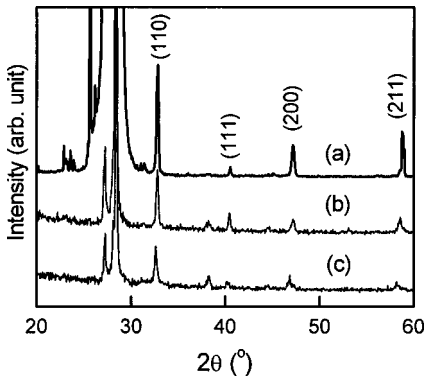

FIG. 2. XRD patterns of the Al_2O_3-doped LSMO thin films derived from targets of: (a) LSMO, (b) 2/10 Al_2O_3-LSMO, and (c) 3/10 Al_2O_3-LSMO.

of Al_2O_3 as an insulator component. It is an extension of our previous work on barium strontium titanate ferroelectric thin films, in which Al_2O_3 was incorporated in order to reduce the dielectric loss tangent of the ferroelectric films for microwave device applications.[19] Our Al_2O_3-LSMO composite thin films showed a maximum LFMR of ~15% at an external magnetic field of 0.3 T.

II. EXPERIMENT

The Al_2O_3-LSMO thin films were deposited on Si (111) substrate, via a pulsed laser deposition (PLD) with a KrF excimer laser at 5 Hz repetition frequency, with an energy density of 270 mJ/pulse. The deposition was conducted for 35 min, at a substrate temperature of 600 °C and a chamber oxygen pressure of 0.2 mbar. The distance between the substrate and target was 4.5 cm. A LSMO target, with a piece of Al_2O_3 on its surface, was used to deposit the Al_2O_3-LSMO thin films. The films with different Al_2O_3 concentrations were deposited from combined targets with different area ratio of Al_2O_3 to LSMO ceramics. A representative target with a certain ratio of Al_2O_3 and BST ceramics is shown in Fig. 1. The area ratio of Al_2O_3 to LSMO was selected to be 1/20, 2/20, and 3/20 in the present study. We also deposited thin films with targets of Al_2O_3 area of 4/20 and more, which led to highly resistive samples and will not be included in the present paper. For comparison, pure LSMO films were also deposited under the same processing condition as the doped ones. LSMO target with a diameter of about 3 cm was prepared via the conventional ceramic processing method, using commercial La_2O_3, $SrCO_3$, and MnO_2 powders as the starting materials. The Al_2O_3 target was a commercially available alumina plate.

The Al_2O_3-LSMO thin films were characterized by x-ray diffraction (XRD) using a Philips PW 1729 type x-ray diffractometer with Cu K_a radiation. The element compositions of the Al_2O_3-LSMO thin films were characterized by Rutherford backscattering (RBS) combined with proton induced x-ray emission (PIXE). In the RBS and PIXE measurement, 2 MeV He^+ particles beam and 2 MeV proton beam were used, respectively. Samples were placed at a scattering angle 150° in IBM geometry. After measuring RBS and PIXE, simulations code RUMP and Dan32 were used to analyses the measuring spectra. The surface microstructure of the deposited Al_2O_3-LSMO samples was examined using a JEOL JSM-6340F type field emission scanning electronic microscope (FESEM). For electrical measurement, four Au dots with a diameter of ~0.3 mm were deposited on the surface of the films as electrodes, using a JOEL magnetic sputtering equipment. The electro-transport and magneto-transport properties were measured using a standard four-probe method with data collected by a personal computer. A maximum ac magnetic field of ~0.3 T was used in the present study.

III. RESULTS AND DISCUSSION

Figure 2 shows the XRD patterns of pure LSMO and the Al_2O_3-LSMO thin films deposited using the targets with different area ratios of Al_2O_3 to LSMO. It is noted that LMSO thin film consists of a single phase of perovskite structure. Its polycrystalline characteristic is evidenced by the strongest diffraction peak of (110). The XRD patterns of the 2/20 and 3/20 Al_2O_3-LSMO are very similar to that of the pure LSMO, except that there is a small peak observed at $2\theta \approx 38°$. This peak has not been identified, which is most likely to be related to the presence of Al_2O_3 in the manganite films. No Al_2O_3 diffraction peak is observed in the XRD patterns, even for the 3/20 Al_2O_3-LSMO sample. This observation could be attributed to the fact that the crystallization temperature of Al_2O_3 is higher than the deposition temperature used in the present study. The exact concentrations of Al_2O_3 in the Al_2O_3- doped LSMO thin films have been determined by RBS, which are listed in Table I. The aluminium concentration is almost linearly proportion to the area ratio of Al_2O_3 in the target, indicating the effectiveness of the combined target deposition.[19] This has been confirmed

TABLE I. Summary of RBS and PIXE measurement.

Area of Al_2O_3 in tatget	1/20	2/20	3/20	4/20	5/20
Al/(Al+Mn) in film (%)	0.46±0.26	1.06±0.16	2.18±0.39	3.09±0.21	4.33±0.45

Downloaded 29 Jul 2004 to 137.132.123.76. Redistribution subject to AIP license or copyright, see http://jap.aip.org/jap/copyright.jsp

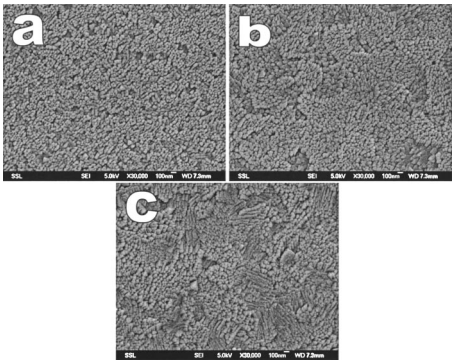

FIG. 3. SEM images of the Al_2O_3−LSMO thin films: (a) LSMO, (b) 1/20 Al_2O_3-LSMO, (c) 3/20 Al_2O_3-LSMO.

by the electro-transport and magneto-transport properties of the Al_2O_3-LSMO composite films, as will be seen later.

Representative surface SEM images of the Al_2O_3 -LSMO thin films are shown in Fig. 3. The pure LSMO thin film is characterized by almost round grains, with an average grain size of less than 100 nm. The microstructures of the 1/20 and 3/20 Al_2O_3-LSMO samples are very similar to that of the pure one. The only difference is that a texturelike microstructure in some areas is observed in the two doped samples, which is probably related to the presence of the Al_2O_3 in the composite films. In addition, the thicknesses of the Al_2O_3-LSMO films were estimated from their cross-sectional SEM images to be ~0.5 μm (not shown here).

Zero-field resistances of the Al_2O_3-LSMO as well as LSMO thin films measured as a function of temperature are shown in Fig. 4. The pure LSMO and 1/20 and 2/120 Al_2O_3-LSMO samples demonstrate a typical metal-insulator transition behavior, while the 3/20 Al_2O_3-LSMO thin film shows an insulator characteristic in the measurement temperature range. The metal-insulator transition temperatures (T_p) of the 1/20 and 2/20 Al_2O_3-LSMO samples are ~229 and ~132 K, respectively, while the T_p value of the pure LSMO is >290 K and that of the 3/20 Al_2O_3 -LSMO film is <77 K. It means that the metal-insulator

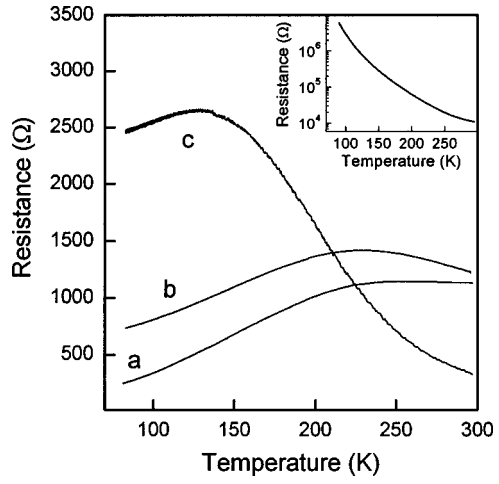

FIG. 4. Zero-field resistance of the Al_2O_3-LSMO thin films as a function of temperature: (a) LSMO, (b) 1/20 Al_2O_3-LSMO, and (c) 2/20 Al_2O_3 -LSMO. Inset is the resistance-temperature curve of the 3/20 Al_2O_3 -LSMO sample.

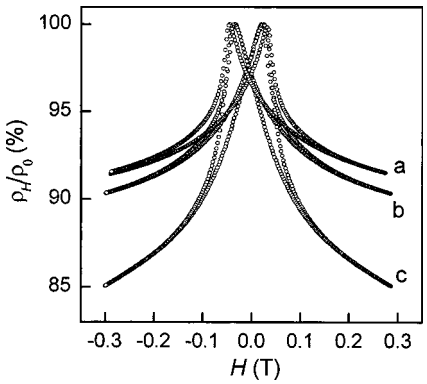

FIG. 5. Magnetoresistance of the Al_2O_3-LSMO thin films as a function of magnetic field at 86 K: (a) LSMO, (b) 1/20 Al_2O_3-LSMO, and (c) 2/20 Al_2O_3−LSMO.

transition temperature of the LSMO thin film decreases as a result of the introduction of Al_2O_3 and further reduces with increasing Al_2O_3 content. In addition to the shift of the T_p value to low temperature, the peak resistance of the Al_2O_3 -LSMO composite films also increases with increasing content of Al_2O_3. Similar observations were reported in other insulator-manganite systems as mentioned in the Introduction,[9–15] which have been well explained in the literatures. In the pure LSMO thin films, the electrical transport is realized through a direct contact between the LSMO grains. This direct contact is diluted/disturbed as a result of the introduction of an insulator. Furthermore, the insulator which is mostly located at the grain boundaries acts a barrier to the electrical transport. Therefore, insulator doped manganites would possess a higher resistivity and lower metal-insulator transition temperature as compared to the undoped ones. With increasing insulator content, the grain boundary will become thicker and thicker. Once a thoroughly insulating grain boundary network forms the composites are completely insulators, and a percolation threshold is defined. In this respect, the percolation threshold of our Al_2O_3-LSMO composite thin films should be close to that of the 3/20 Al_2O_3-LSMO sample (Al/Al+Mn~2.18%). This value is much less than that observed in bulk ceramic composites.[10–15]

Magnetoresistances of the thin films as a function of magnetic field at a temperature of 86 K are shown in Fig. 5. It is demonstrated that the maximum LFMR values at an external magnetic field of ~0.3 T of the pure LSMO, 1/20 and 2/20 Al_2O_3-LSMO samples are 9%, 10%, and 15% respectively. The maximum LFMR of the 2/20 Al_2O_3-LSMO thin film of 15% is comparable with that of $(La_{0.7}Sr_{0.3}MnO_3)_{0.9}(MgO)_{0.1}$ thin film via sol-gel (H =0.4 T, T=4.2 K),[16] partially crystallized $La_{0.5}Sr_{0.5}MnO_3$ thin film via PLD(H=0.4 T, T=77 K) and most of the ceramic bulk composites.[10–15] This enhanced LFMR of our Al_2O_3-LSMO thin films can be similarly interpreted by the mechanism of spin-polarized tunneling through manganite/insulator/manganite junction structures, which has been widely used in the literatures.

As discussed earlier, it has been acknowledged that large variations in the resistance at low temperatures in polycrystalline manganites, as a result of the application of a low

Downloaded 29 Jul 2004 to 137.132.123.76. Redistribution subject to AIP license or copyright, see http://jap.aip.org/jap/copyright.jsp

external magnetic field of the order of the coercive field H_C, is an extrinsic property of the manganites, which is due to the presence of the high values of spin polarization[6] and most likely pinning of domain walls at the grain boundaries.[7] Hence, artificial grain boundary effect can be realized by proper incorporation of dopant into manganites. This well explains the experimental observations of our Al_2O_3-LSMO thin films. Introducing Al_2O_3 into LSMO created artificial grain boundaries. Therefore, the $1/20$ Al_2O_3-LSMO film has a larger LFMR than the pure LSMO sample and the LFMR effect increases with increasing content of Al_2O_3 before percolation.

The enhanced LFMR effect, together with the electrotransport properties of the Al_2O_3-LSMO thin films, can be taken as a good support that our combined Al_2O_3-LSMO target configuration is a very effective way to deposit the Al_2O_3-LSMO composite thin films. Moreover, the composition of the Al_2O_3-LSMO thin films can be further tuned by the target arrangement. Similar results were obtained for Al_2O_3-LSMO thin films deposited on Si (100) and $LaAlO_3$ substrates (not shown). It is believed that this method can be readily extended to the combinations of other manganites and insulations.

IV. CONCLUSIONS

Enhanced LFMR effect has been realized in $La_{0.7}Sr_{0.3}MnO_3$(LSMO) thin films by the addition of Al_2O_3, via the PLD method. A maximum LFMR of 15% was achieved in the $3/20$ Al_2O_3-LSMO composite thin films, where the Al/Al+Mn was ~2.18%. This technique should also be applicable to other manganites and insulators.

[1]S. Jin, T. H. Tiefel, M. McCormack, R. A. Fastnacht, R. Ramesh, and L. H. Chen, Science **264**, 413 (1994).
[2]R. Von Helmolt, J. Wecker, B. Holzapfel, I. Schultz, and K. Samwer, Phys. Rev. Lett. **71**, 2331 (1993).
[3]K. Chahara, T. Ohno, M. Kasai, and Y. Kozono, Appl. Phys. Lett. **63**, 1990 (1993).
[4]Y. Okimoto, Y. Tomioka, Y. Onose, Y. Otsuka, and Y. Tokura, Phys. Rev. B **57**, R9377 (1998).
[5]P. Schiffer, A. P. Ramirez, W. Bao, and S. W. Cheong, Phys. Rev. Lett. **75**, 3336 (1995).
[6]J. H. Park, E. Vescovo, H. J. Kim, C. Kwon, R. Ramesh, and T. Venkatesan, Nature (London) **392**, 794 (1998).
[7]J. B. Philipp, C. Hofener, S. Thienhaus, J. Klein, L. Alff, and R. Gross, Phys. Rev. B **62**, R9248 (2000).
[8]S. Gupta, R. Ranjit, C. Mitra, P. Raychaudhuri, and R. Pinto, Appl. Phys. Lett. **78**, 362 (2001).
[9]L. E. Hueso, J. Rivas, F. Rivadulla, and M. A. Lopez-Quintela, J. Appl. Phys. **89**, 1746 (2001).
[10]D. Das, A. Saha, S. E. Russek, R. Raj, and D. Bahadur, J. Appl. Phys. **93**, 8301 (2003).
[11]Ll. Balcells, A. E. Carrillo, B. Martinez, and J. Fontcuberta, Appl. Phys. Lett. **74**, 4014 (1999).
[12]S. Valencia, O. Castano, J. Fontcuberta, B. Martinez, and Ll. Balcells, J. Appl. Phys. **94**, 2524 (2003).
[13]D. K. Petrov, L. Krusin-Elbaun, J. Z. Sun, C. Field, and P. R. Duncombe, Appl. Phys. Lett. **75**, 995 (1999).
[14]O. A. Shlyakhtin, K. H. Shin, and Y. J. Oh, J. Appl. Phys. **91**, 7403 (2002).
[15]Z. C. Xia *et al.*, Solid State Commun. **128**, 291 (2003).
[16]S. A. Koster, V. Moshnyaga, K. Samwer, O. I. Lebedev, G. van Tendeloo, O. Shapoval, and A. Belenchuk, Appl. Phys. Lett. **81**, 1648 (2002).
[17]V. Moshnyaga *et al.*, Nat. Mater. **2**, 247 (2003).
[18]J. M. Liu *et al.*, Appl. Phys. Lett. **76**, 2286 (2000).
[19]K. B. Chong *et al.*, J. Appl. Phys. **95**, 1416 (2004).

Downloaded 29 Jul 2004 to 137.132.123.76. Redistribution subject to AIP license or copyright, see http://jap.aip.org/jap/copyright.jsp